CONF-790655--2

DESIGN AND PERFORMANCE OF THE DRAG-DISC TURBINE TRANSDUCER

R. H. Averill, L. D. Goodrich,
R. E. Ford
EG&G Idaho, Inc.
P.O. Box 1625
Idaho Falls, Idaho 83401

ABSTRACT

Mass flow rates at the Loss-of-Fluid Test (LOFT) facility, EG&G Idaho, Inc., at the Idaho National Engineering Laboratory, are measured with the drag-disc turbine transducer (DTT). Operational description of the DTT and the developmental effort are discussed. Performance data and experiences with this transducer have been evaluated and are presented in this paper.

1. INTRODUCTION

In the LOFT Experimental Program, the mass flow rate through the reactor core and the reactor piping is measured at several locations. This measurement is complicated by the fact that during the transient, the fluid becomes a nonhomogeneous mixture of liquid water and steam at, or very near saturation. In addition, materials from which the transducer is fabricated must be carefully chosen for their ability to survive the destructive effects of the water chemistry and radiation. One of the transducers used to measure the mass flow rate in the reactor at LOFT consists of a drag disc and turbine combination. The design and performance of this drag-disc turbine transducer are the subjects of this paper.

2. DESIGN

In LOFT, the mass flow rate is not measured directly but is derived from velocity and momentum flux data taken within the primary coolant system. Coolant velocity is obtained from the output of the turbine flowmeter, and momentum flux (ρv^2) is obtained from the drag disc. These two transducers are combined into the drag-disc turbine transducer. To calculate the mass flow rate using these transducers, the momentum flux is divided by the fluid velocity and multiplied by the known cross-sectional area.

2.1 Principle of Operation

As fluid flows through the DTT, the rotational speed of the turbine is monitored by an eddy-current transducer (ECT) coil mounted near the turbine blade tips. The coil produces an output pulse each time a turbine blade tip passes the coil, the pulse rate being dependent on the rotational speed of the turbine which is a function of the coolant velocity.

The drag disc responds to the coolant momentum flux and to the flow direction. The displacement of the drag disc is measured by a variable reluctance transducer (VRT) which is comprised of a coil with a slug passing freely through its center. As the drag disc is displaced by the flow, the slug is displaced in the coil, thereby changing the output of the coil.

2.2 Design Philosophy

The DTT must not only function properly, it must do so while immersed in the primary coolant. Prior to a blowdown, the DTT experiences a single-phase, uniform fluid flow at high temperatures and pressures. During the blowdown, the flow is two-phase and not uniform but is stratified, laminar, or slug.

Although other types of transducers are exposed to this environment, the DTT is the only transducer with moving parts in the coolant. In addition, when the DTT is mounted in the piping locations, it is cantilevered in the pipe. Because of these conditions, the DTT has unique functional and survivability design problems.

2.2.1 Early DTT Design. Early attempts to solve these unique design problems led to a DTT consisting of a single body design that supported the turbine and drag-disc and containing the ECT and the VRT coils. This body was machined from a Type 304L stainless steel block, into which cavities were bored to contain the coils. Access covers were welded to the body to protect the coils from the primary coolant. The turbine shaft assembly was supported by two posts, each of which contained a gold bearing. The drag-disc/torsion bar assembly was housed in the forward end of the body with a horizontal shaft transmitting the motion of the drag disc to the VRT at the aft end of the body. A Type K thermocouple was located on the DTT to monitor fluid temperature. The shroud, end caps, and cover plates were welded to the body to complete the drag-disc turbine assembly. The shroud and end caps were provided to act primarily as a flow straightener/homogenizer, but performed the secondary function of containing component parts in the event of a structural failure during test operation.

The approximate overall dimensions of the DTT were: (a) depth - 6.4 cm (b) width - 3.8 cm, and (c) length - 12 cm. The finished assembly was mounted to various supporting structures by means of socket head caps screws that threaded into the transducer body.

2.2.2 Modular DTT Design. Due to several problems with the early DTT, the design has evolved from a single body, fully welded DTT, to the present concept. The function of the turbine and drag disc have remained the same, but there have been significant modifications in their configuration.

The present design is a modular construction, that is, the drag disc and turbine are individual modules which are interchangeable. The purpose of this design is to facilitate assembly and repair of the DTT. When fully assembled as shown in Figure 1, the visible components of the DTT are the drag-disc module, the turbine module, the shroud, and the forward and aft end caps. By removing the end caps and the shroud from the DTT, the transducers, shown in Figure 2, are exposed. Normal fluid flow is from the drag disc to the turbine.

The thermocouple is now positioned downstream of the turbine. As in the early design, a Type K thermocouple is used to measure the temperature of the fluid.

The modular DTT is not welded, but securely bolted. All bolts are locked in place by pinning, welding, or both. The overall dimensions of the DTT have been maintained to provide continuity of the supporting structures.

2.3 Detailed Design

In discussing the design details, a comparison between the early and modular DTT is given where there have been significant changes. This has been done for two reasons: (a) early DTTs are still installed at LOFT and (b) to indicate how the design has evolved. For convenience, the detailed design has been divided into three parts; (a) the turbine, (b) the drag disc, and (c) the final assembly of the DTT.

2.4 Turbine Transducer Design

A turbine transducer, shown in Figure 3, consists of these major components: (a) the turbine, (b) two journal bearings, (c) an eddy-current transducer, and (d) the transducer body. Not considered part of the turbine transducer but required for its operation is the signal conditioning electronics. The following is a discussion of the major components including the electronics.

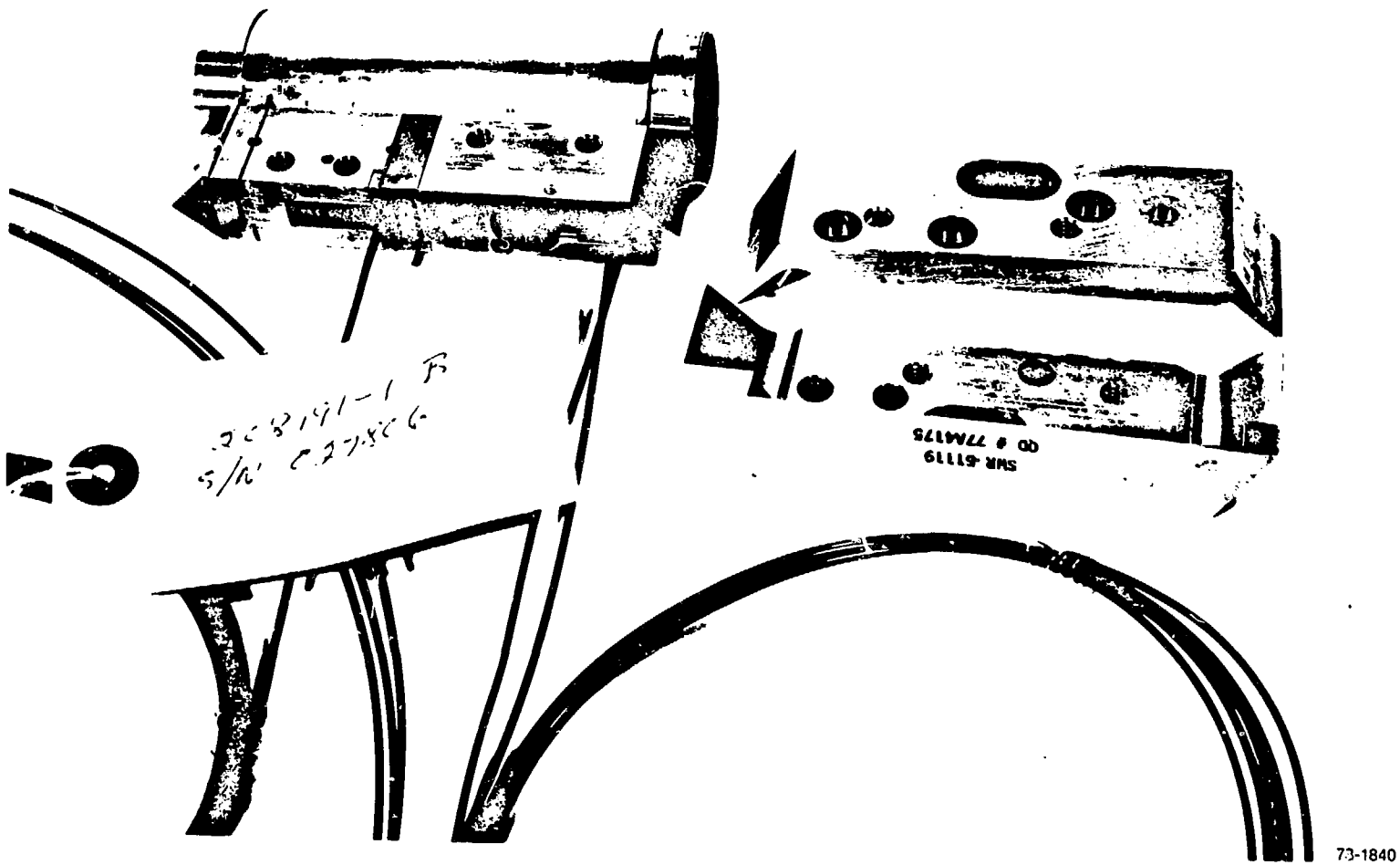

Fig. 1 Drag-disc turbine transducer completed assembly.

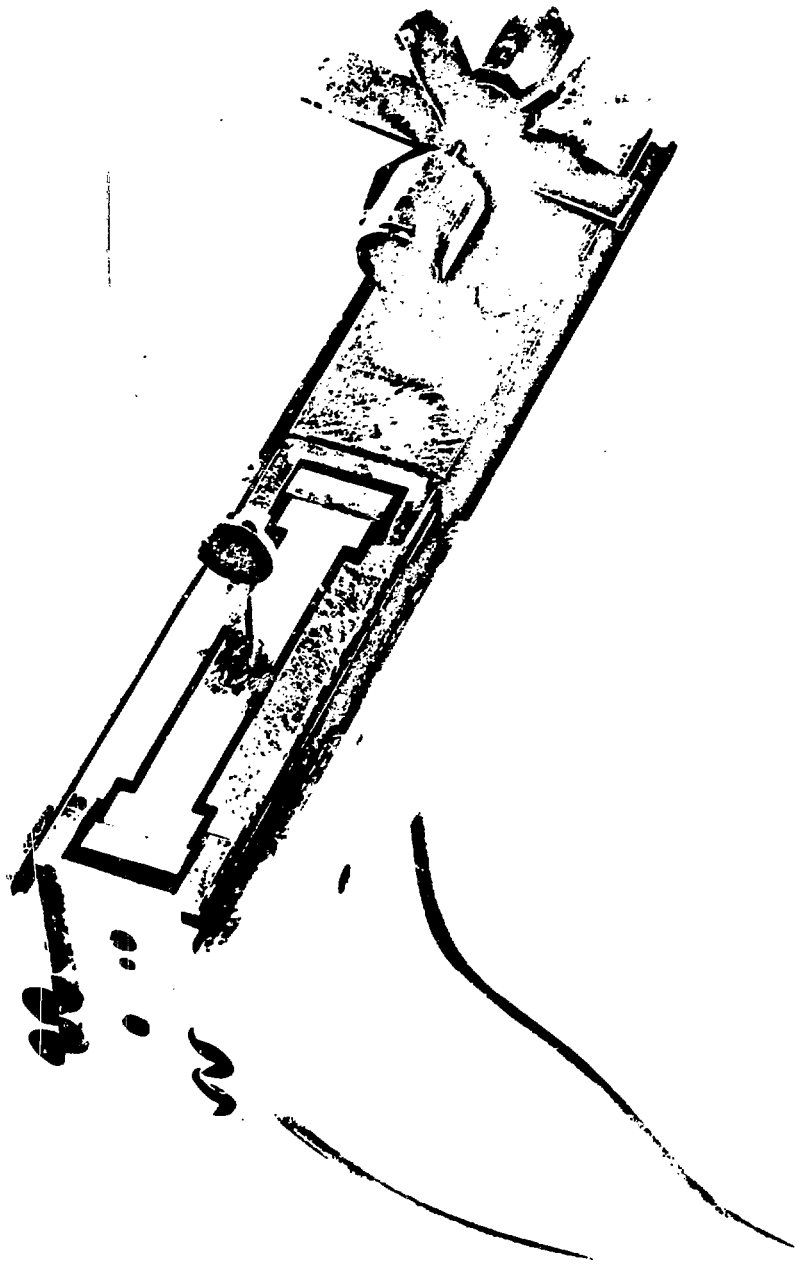

77-62??

Fig. 2 Partially assembled drag-disc turbine transducer.

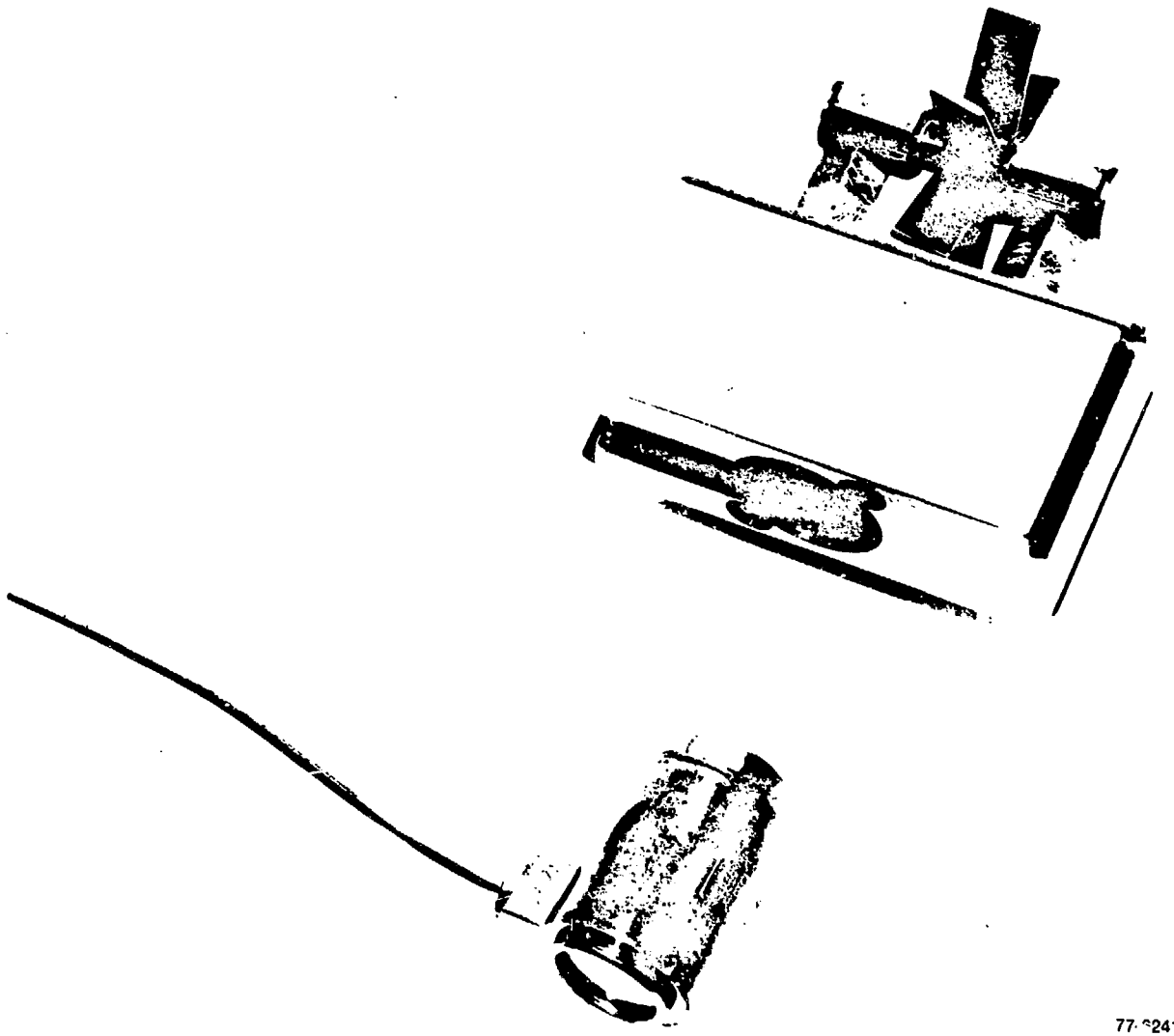

77-8241

Fig. 3 Turbine transducer.

2.4.1 Turbine. The turbine consists of six twisted blades mounted on a shaft, as shown in Figure 4. The turbine is a 17-4 pH investment casting pressed onto a shaft. The early shaft was also 17-4 pH; but due to oxidation of the shaft, it has been changed to 440C stainless steel which is more corrosion resistant. For any given turbine range, the blade angle is such that the $\frac{\tan\phi}{R}$ is a constant, where ϕ is the angle between the normal axis and the blade at any given radius R along the blade. For different turbine ranges, a new and therefore a different blade angle is calculated.

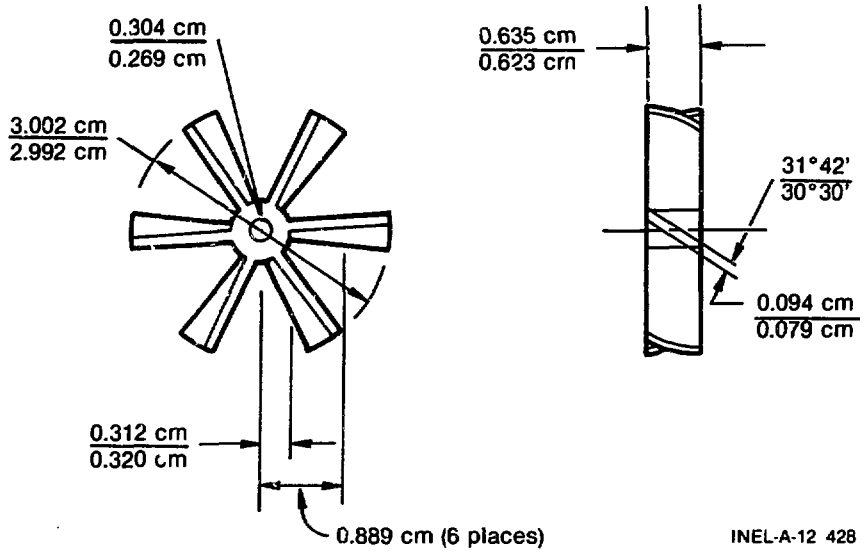

Fig. 4 Turbine blade geometry.

2.4.2 Journal Bearings. The bearing design consists of bushing and thrust bearings (see Figure 5). The early bearing design used two gold alloy journal bearings machined to very close tolerances. The close tolerances maintain the rotating turbine properly positioned over the coil, preventing a loss of sensitivity in the measurement. These bearings carry the radial and axial loads generated by the turbines and are designed to withstand the chemical, thermal, and radiation environment of the reactor.

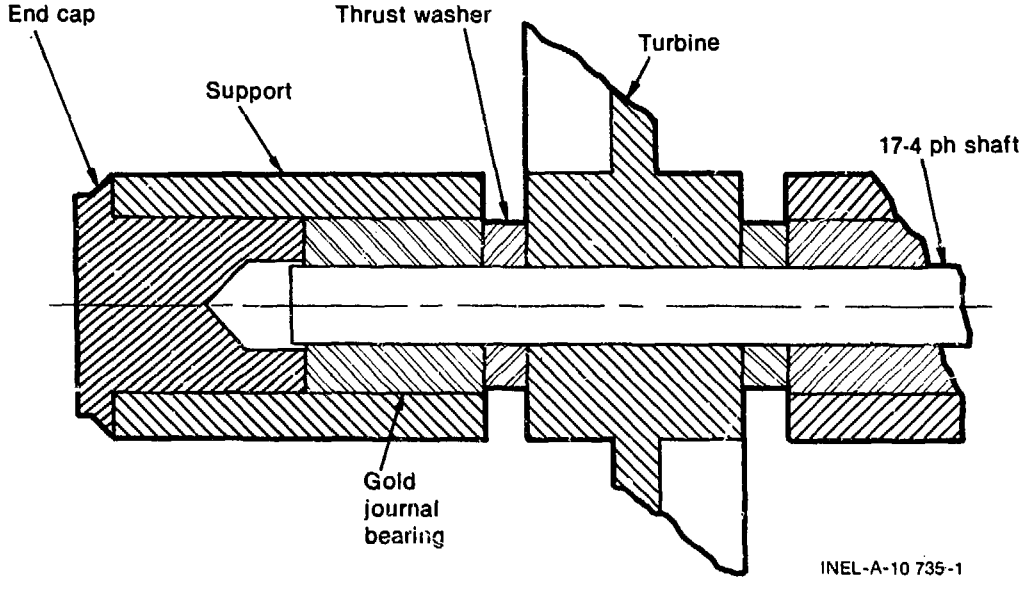

Fig. 5 Diagram of early bearing configuration.

These turbines would seize due to two problems: (a) crevice corrosion between the bushing and shaft and (b) post misalignment due to stress relieving the posts at operating temperatures. To eliminate these problems, the turbine transducer was redesigned to incorporate self-aligning graphite bearings, shown in Figure 6. Tests have shown that graphite bearings on a 440C stainless steel shaft do not bind after 2500 hours of flow and more than six weeks of soak time at LOFT temperatures and pressures using borated water.

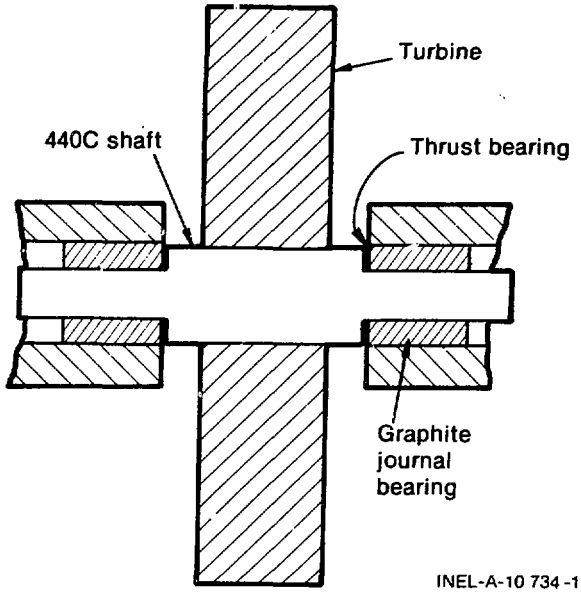

Fig. 6 Diagram of graphite bearing configuration.

2.4.3 Eddy-Current Transducer. An eddy-current transducer (ECT) coil is used to measure the rotational speed of the turbine. The ECT coil is housed in the body directly below the turbine and forms half of a bridge network. The other half of the bridge is contained in a signal conditioning electronics package.

The eddy-current coils are wound with high-temperature ceramic insulated silver alloy wire and are vacuum fired. The coil is then placed in the coil housing with three coil leads exposed (see

Figure 7). The coil leads are then laser welded to the signal cable. The coil and leads are potted to prevent damage to the assembly. The housing is positioned in the body of the module. A 0.254-mm, stainless steel diaphragm forms the seal between the sensing coil and the turbine blade tips.

2.4.4 Turbine Transducer Body. The turbine transducer body is machined from a Type 304L stainless steel block. The aft turbine post is an integral part of the body, but the forward support post is removable to facilitate assembly. This post is bolted and pinned to the body. The coil assembly is housed in a cavity in the body and is secured by machine screws. The bearings and turbine/shaft are captive in the posts. All screws are secured to the body by pinning and/or welding.

2.4.5 Turbine Signal Conditioning. The ECT electronics circuitry consists of an oscillator or driver, one-half the bridge network (the other half is the ECT coil), and an amplifer-converter for conditioning the bridge output. All components and wiring on the unit circuit board are isolated from the metal container, and the two transformers at the bridge isolate the bridge and the transducer from circuit board common. Thus, the output from the unit is able to be connected to signal-recording ground without ground-loop problems. Figure 8 is a block diagram of the turbine readout amplifier.

The oscillator serves to drive the bridge formed by resistors and the coil. With the coil between two of the turbine blades and the bridge properly balanced by adjusting the null and phase, the fundamental frequency bridge output is approximately zero. As a turbine blade is brought near the coil, the blade causes a reflected-impedance change in the coil and thus unbalances the bridge. During the time a blade is near the coil, a bridge output with large fundamental frequency content occurs. Since the fundamental frequency (100 kHz) is much larger than the frequency of rotation of the turbine, the 100-kHz signal will be modulated with an envelope which has peak amplitude for each passage of a turbine blade.

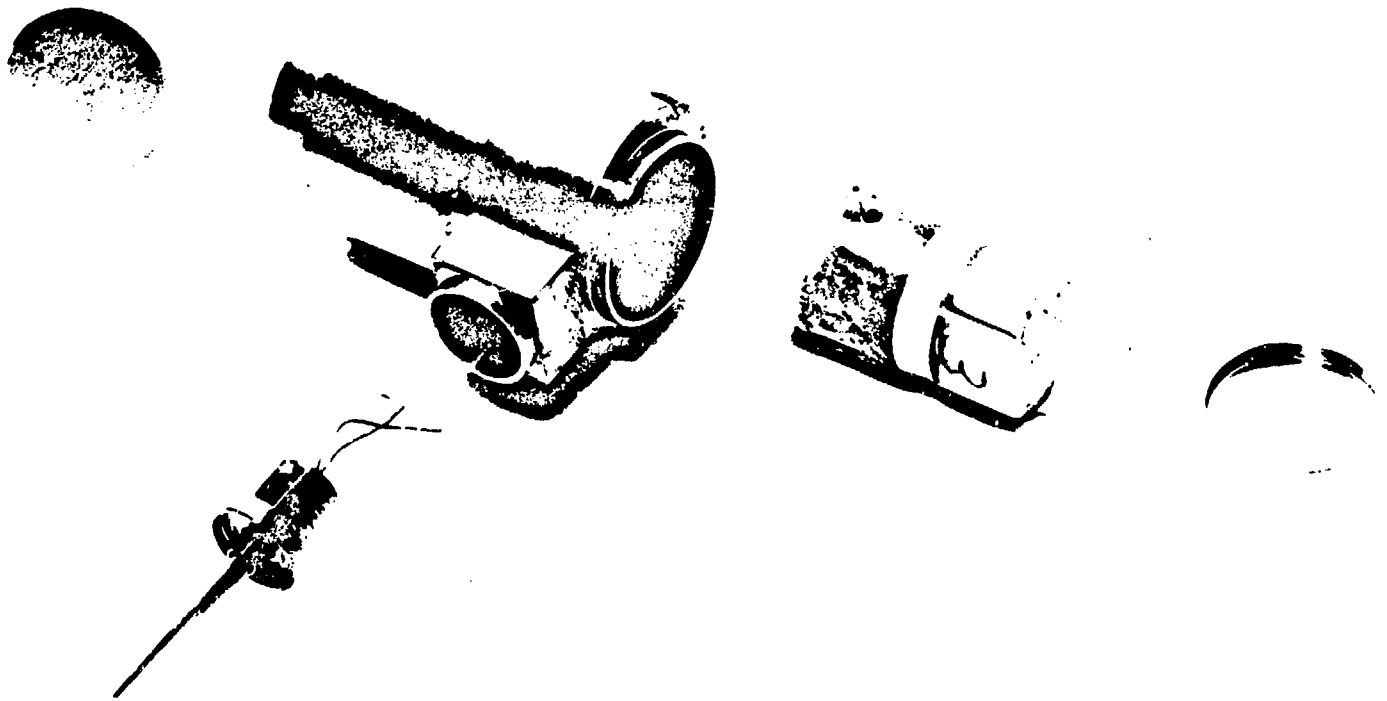

77-6245

Fig. 7 Turbine coil.

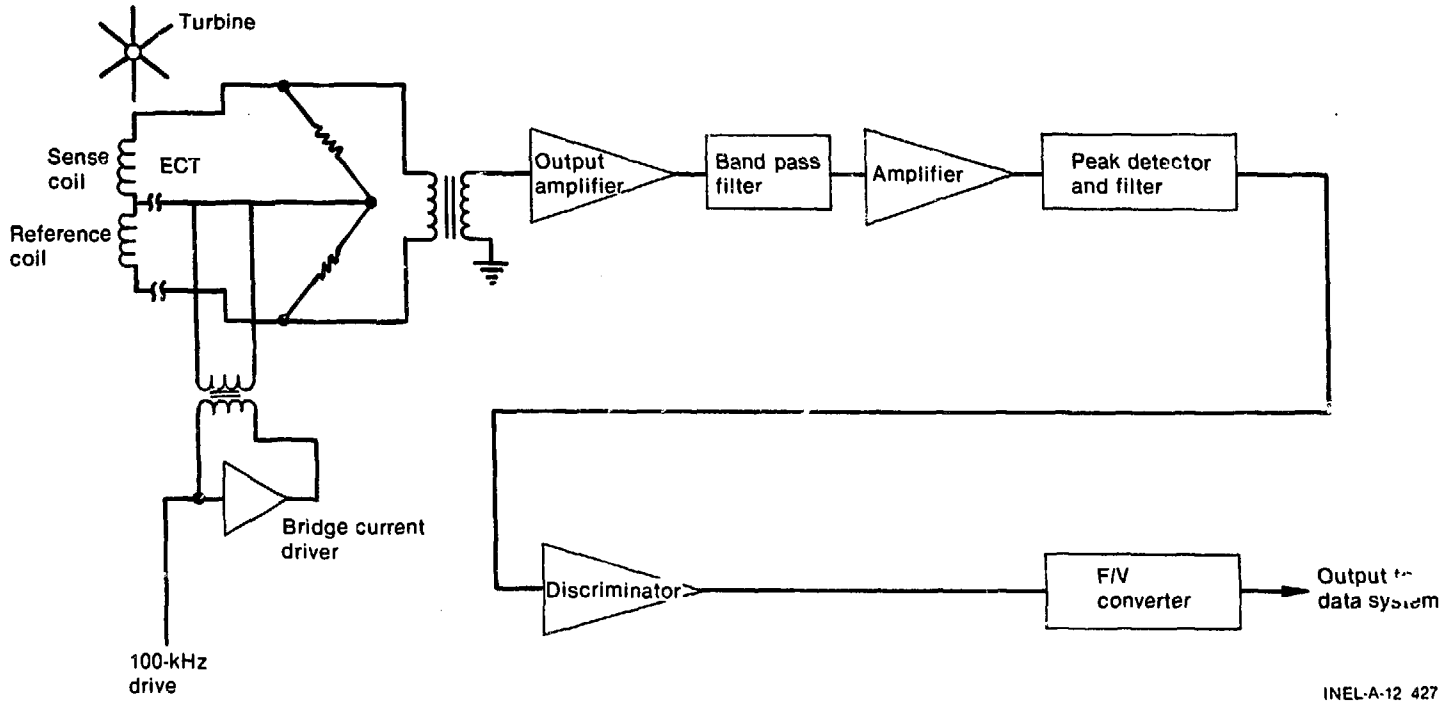

Fig. 8 Turbine readout amplifier block diagram.

The amplifier-converter amplifies and filters the bridge output. The signal is then full wave rectified, which results in an envelope frequency with a 200-kHz ripple. The 200-kHz ripple is filtered out and the resultant frequency is equal to the rate at which turbine blade passages occur The discriminator then triggers each time the RC integrated envelope rises above a given level. The output of the discriminator yields a pulse output for each blade passage. The dc output, proportional to the rpm of the turbine, is obtained by using a frequency-to-dc converter module. The operational amplifier furnishes a low impedance output from the frequency-to-dc converter.

2.5 Drag-Disc Design

The drag disc, as shown in Figure 9, consists of: (a) the drag body (a target and pedestal), (b) torsion or leaf springs, (c) variable reluctance transducer, and (d) the transducer body. As in the turbine transducer, the signal conditioning electronics is not part of the transducer but is required for its operation. The following is a discussion of the major components and the associated electronics.

2.5.1 Drag Body. The target, or circular disc plate, is machined from Type 304 stainless steel. The thickness of the target is approximately 0.1 cm, but the diameter varies from 0.76 to 1.4 cm, depending upon the desired range. The target is welded to a pedestal and positioned such that the target is in the center of the shroud. This assembly forms the drag body.

The force with which the fluid strikes the drag body is proportional to the momentum flux. The force on the drag body is given as

$$F = \frac{1}{2} \rho v^2 C_d A \qquad (1)$$

where

ρ = density of fluid

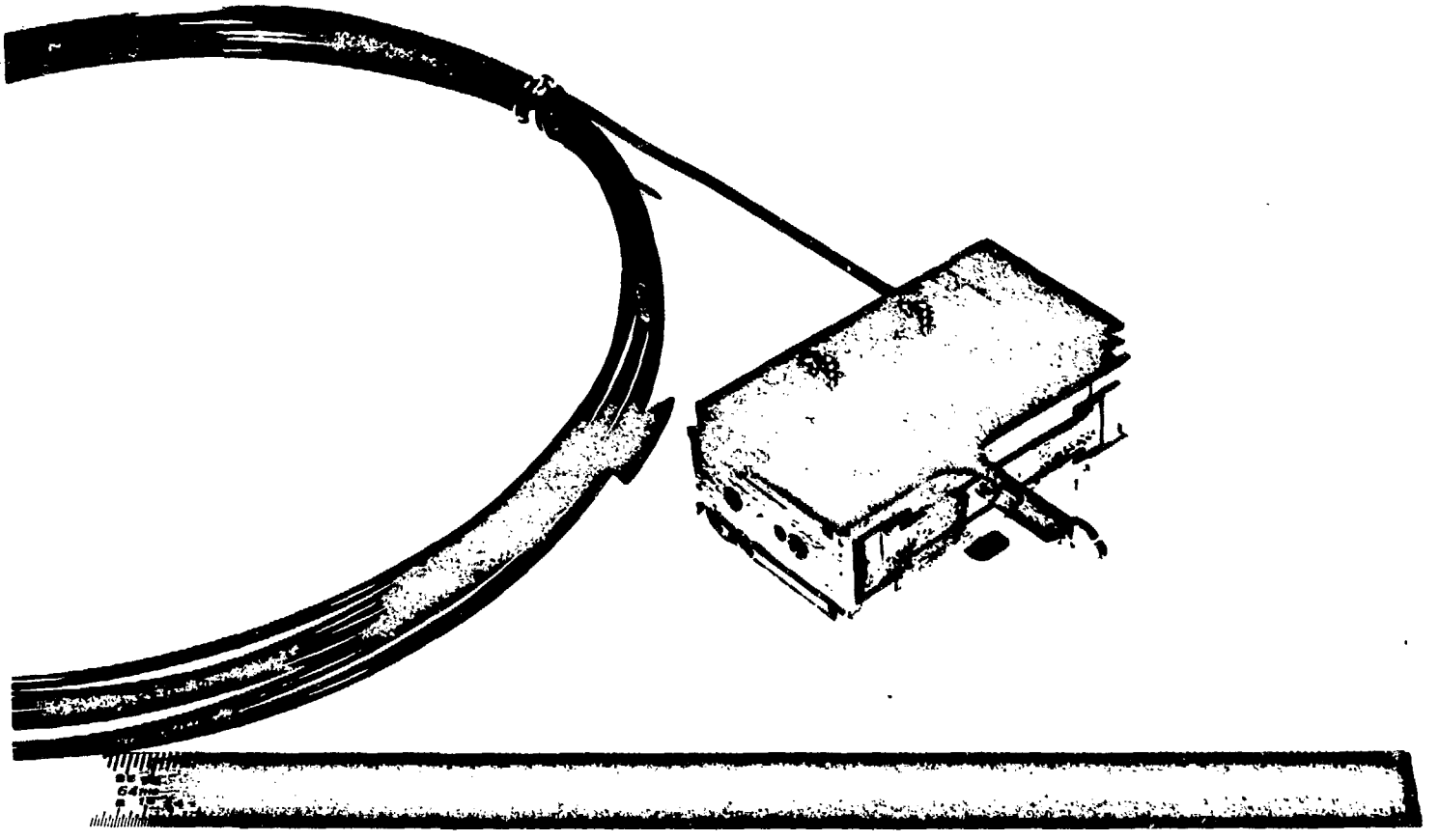

78-1844

Fig. 9 Drag-disc transducer.

v = velocity

C_d = drag coefficient

A = area of target.

The drag coefficient, C_d, is a function of Reynolds number, as shown in Figure 10. The circular plate chosen has essentially a constant C_d of 1.17 above a Reynolds number of 10^4 (Figure 10). Since all operations in LOFT are at Reynolds numbers above 10^4, the circular plate is a satisfactory geometry for the target. The arm (or pedestal) that holds the target in place must also be insensitive to Reynolds numbers over the expected operating range.

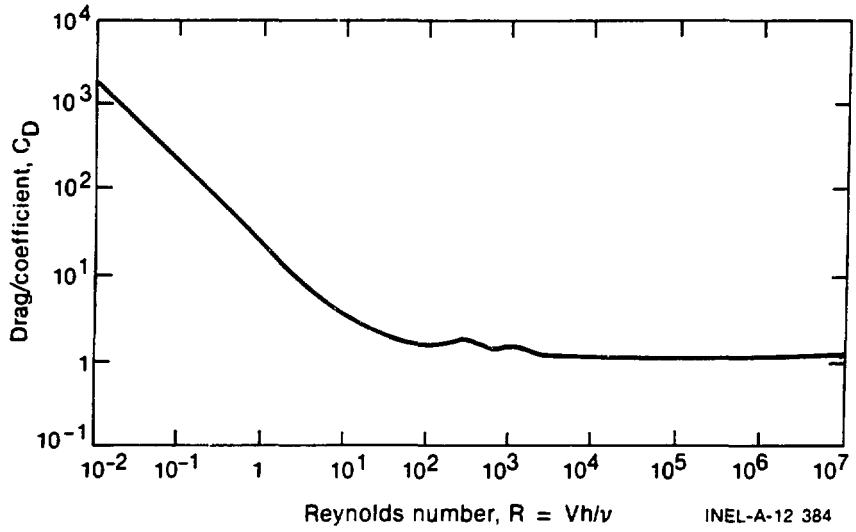

Fig. 10 Drag coefficient of circular and square plates (in normal flow) as a function of Reynolds number.

2.5.2 Springs. The early DTT design used a torsion bar for a spring as shown in Figure 11. The target was welded to an arm which, in turn, was welded to the torsion bar. A shaft was attached to the torsion bar and extended underneath the entire length of the DTT

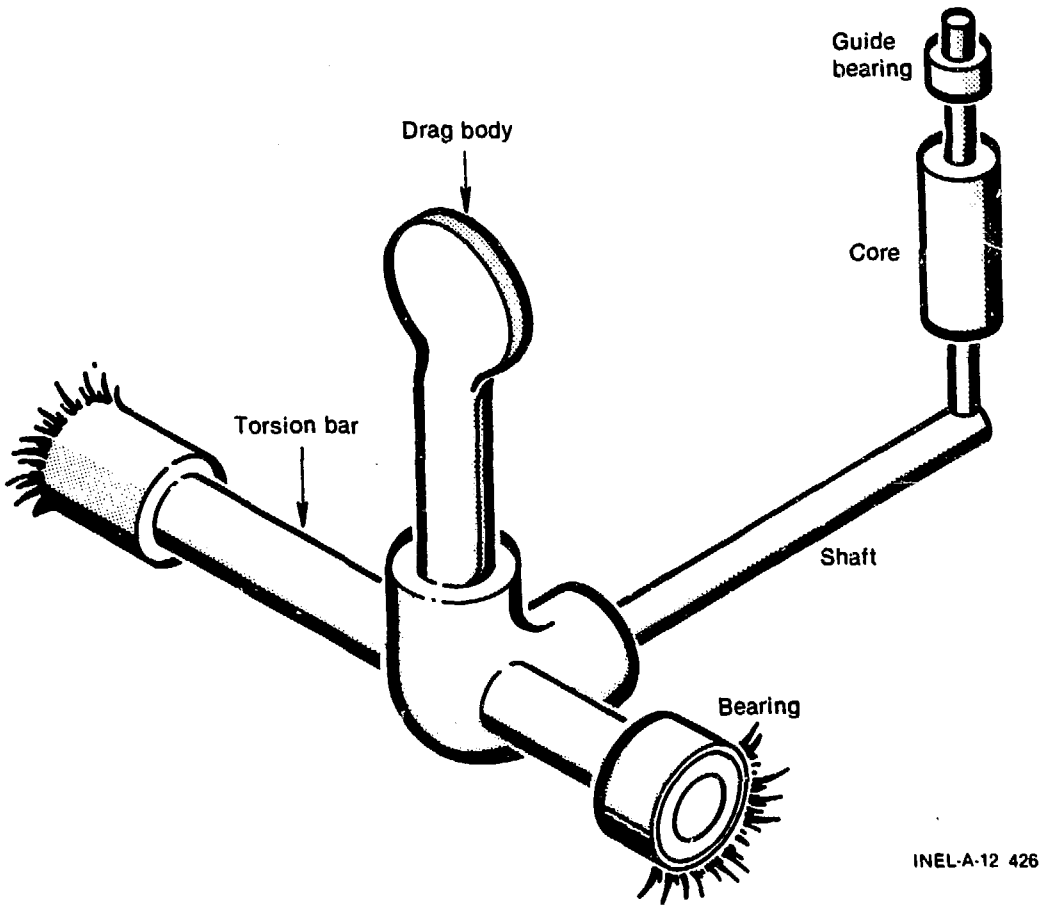

Fig. 11 Torsion spring drag disc.

body exposed to the fluid environment. Welded to the shaft was the core which extended vertically into the DTT body and through the coil. The uppermost part of the core was held in position by a guide bearing.

Two problems that existed with this design were (a) excessive stiction of the core at the guide bearing and in the coil and (b) the drag coefficient for the arm that supported the target was not a constant over the desired ranges and because the cross-sectional area of the arm was equal to that of the target, useful calibration data were difficult to obtain.

The modular design incorporated leaf springs into the drag disc, thus eliminating the torsion bar (see Figure 12). The springs are clamped in a fixed position at the lower end and bolted to the carrier of the drag body at the upper end. The arm has been replaced by a thin pedestal which has a constant drag coefficient in the drag-disc operating ranges. The core is rigidly mounted to the carrier by a core clamp and passes freely through the center of the coil. The coil is positioned horizontally in the modular design and it was this change that enabled the development of the modular concept.

2.5.3 Variable Reluctance Transducer. A variable reluctance transducer (VRT) is used to detect mechanical displacement of the drag body. The VRT coil is housed in the drag-disc module and forms half of a bridge network much like that of the ECT coil of the turbine module. As in the ECT coil, the other half of the bridge is formed by the signal conditioning electronics.

The fabrication process is similar to the ECT coil, but the coil wire is a platinum alloy instead of a silver alloy.

The early core was machined from one piece of 17-4 pH stainless steel. But, due to corrosion buildup which caused the sticking problem discussed earlier, the core was redesigned to reduce the amount of

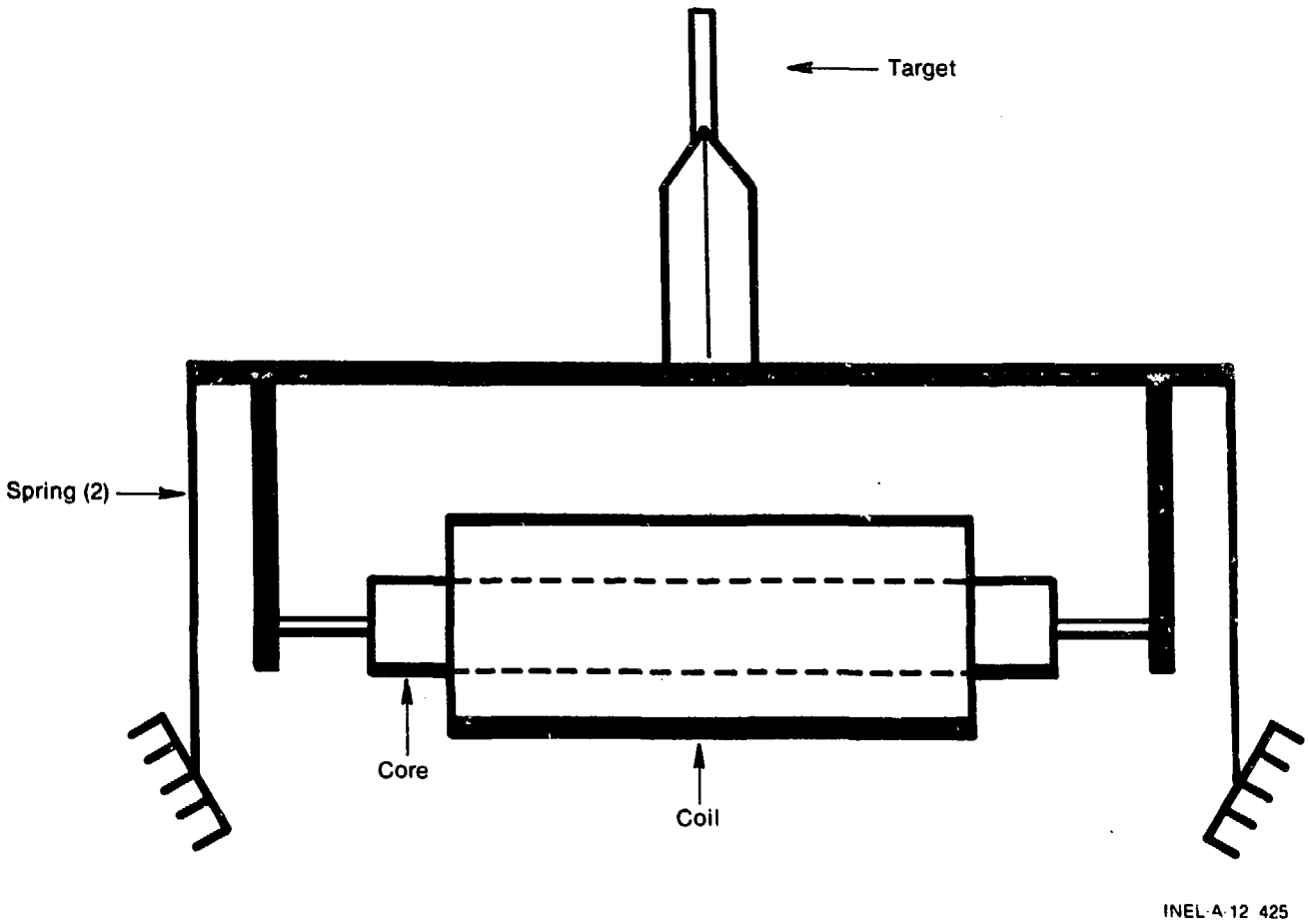

Fig. 12 Leaf spring drag disc.

17-4 pH. New cores are hollow cylinders machined from 17-4 pH and welded onto a 304 stainless steel rod.

2.5.4 Drag-Disc Transducer Body. The drag-disc body, like that of the turbine, is machined from a Type 304L stainless steel block. Cavities are bored into the body to contain the VRT coil and springs, shown in Figure 13.

The assembly is performed in the following sequence: the drag body is welded to the pedestal, the pedestal is welded to the carrier, and the springs are bolted to the carrier.

The coil is then positioned in a cavity in the body and pinned in place. Next, the core is slipped into the coil. The preassembled drag body carrier is lowered onto the core, and the core is clamped to the carrier. The lower ends of the springs are clamped in position with the two end blocks and bolted to the drag-disc body.

2.5.5 Drag-Disc Signal Conditioning. The VRT coil is driven in a bridge configuration with a 3.127-kHz sinusoidal current. When the drag disc is at rest so that the core is in the center of the coil, the bridge can be balanced for minimum output. As the core is displaced, the output of the bridge changes both in amplitude and phase. This output is amplified and filtered, and the resultant output is a dc voltage level proportional to the drag-disc displacement. Because the system is phase sensitive, direction of the flow can be determined by the polarity of the output.

Figure 14 is a block diagram of the VRT output signal conditioner. All units are supplied with a low impedance 5.00 V root-mean-square (rms) 3.125-kHz sinusoidal carrier voltage. An active voltage-to-current converter with a gain of $2\sqrt{2}$ mA/V (5.00 V rms results in a 10-mA peak current) drives the VRT bridge.

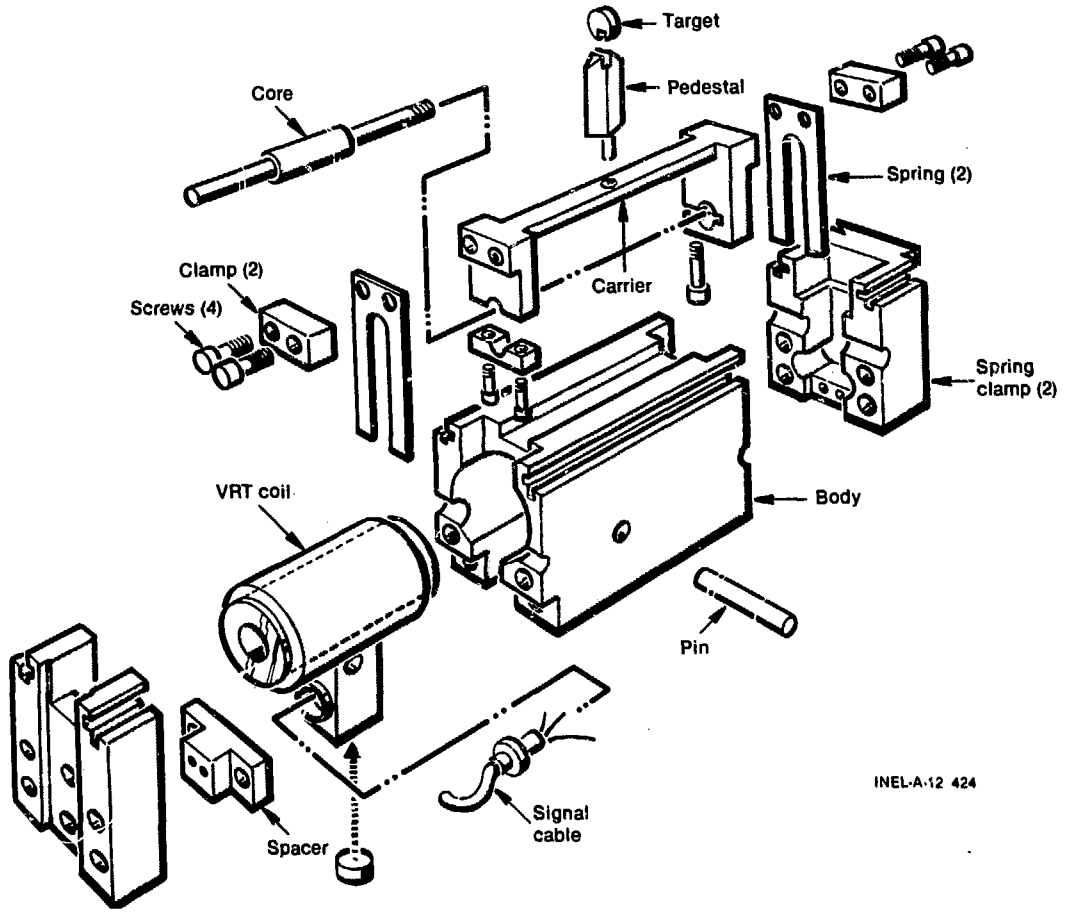

Fig. 13 Exploded view of drag disc.

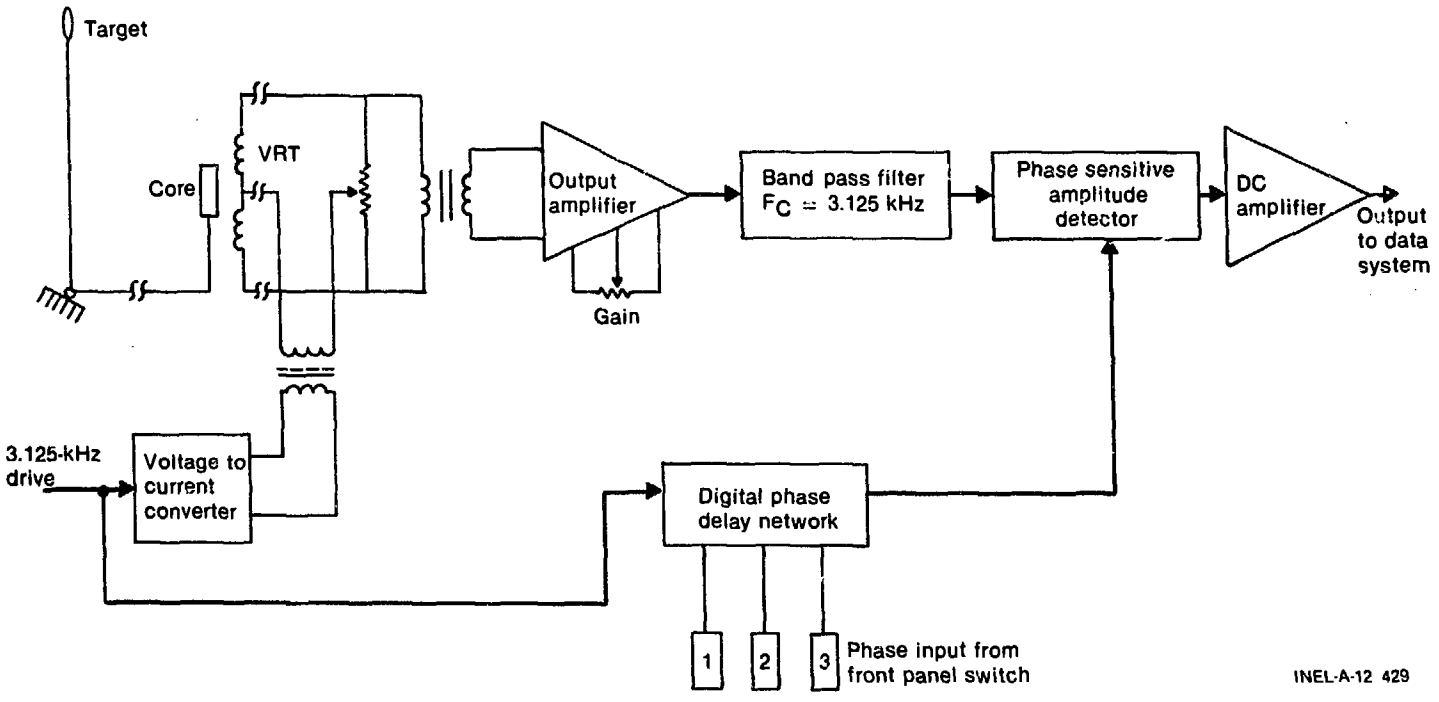

Fig. 14 Drag-disc output signal conditioner block diagram..

The bridge amplifier output is fed to a two-stage, four-pole active band pass filter with an f_c = 3.127 kHz. This filter has unity gain at f_c and is intended to reject 60 Hz (-58 dB) and high frequency noise from other carrier sources.

The band pass filter is followed by a full wave phase sensitive amplitude detector. It is, in effect, a two-quadrant multiplier. Following the multiplier on the detector board is a 300-Hz Butterworth low-pass filter to remove the second harmonic component of the output.

The reference signal to the detector is delayed by a phase (in degrees). Its value is determined by a resistance inserted in series with one side of the VRT at the bridge completion board in the signal conditioner. The phase delay is then changed until no change in dc output occurs. This is a first-order compensation technique to make the measurement less sensitive to change in series line resistance in the wiring to the VRT.

An output isolation amplifier follows the detector and serves two purposes. First, the amplifer provides a low impedance drive to the output; second, its output is configured so that it can drive a load with a relatively large capacitive component without becoming unstable.

2.6 Final DTT Assembly

The drag-disc module, the turbine module, and both end caps are dovetailed in the modular concept. In addition, the modules have a set of channels along the top used in mounting the shroud. Final assembly is performed by sliding the modules together at the dovetails, press fitting the shroud through the channels on each module, and then slipping the end caps in place. The end caps are then secured with bolts, and the bolts are pinned in place.

3. CALIBRATION

Drag-disc turbine transducers are calibrated before installation at LOFT. Calibration data are then correlated with other parameters to determine the functional relationships between systematic errors and variables other than those the instrument was designed to measure. These error functions were then represented by mathematical equations (usually in the form of polynominals of degree five or less) and incorporated in the data reduction program. Individual turbine flowmeters and drag discs are calibrated in single-phase water at ambient temperatures. This calibration is performed with all the fluid flow going through the DTT. After the DTTs are mounted on a support structure called a rake, the temperature sensitivity is quantified by installing the rake in the Fast Loop at LOFT Test Support Facility (LTSF). The rake is tested at four or five temperatures. After installation in LOFT, these calibrations are checked using the data from the single-phase water variable frequency pump tests, that is, the mass flow rate is varied by changing pump speed. The intact loop venturi data are used as the mass flow rate reference. The venturi meter data are then used to calculate average velocities and momentum fluxes in the intact loop and the reactor vessel. These calculated quantities are subsequently compared to the measured turbine velocities and drag-disc momentum fluxes to verify or provide changes to the respective instrument calibration equations.

3.1 Turbine Equations

The single-phase water calibration equation for the turbine is

$$u = D_0 + D_1 V(t) \qquad (2)$$

where

u = velocity

D_0 = zero offset

D_1 = calibration coefficient

$V(t)$ = voltage output at time t.

Currently, the single-phase equation is used for LOFT mass flow rate calculations. This equation has been used due to lack of knowledge of the local void fraction. A series of tests is planned for performance at Wyle Laboratories which are to extract the local void fraction from the three-beam densitometer. With the knowledge of the local void fraction and the assumption that the local slip is unity, then correction of the turbine data is possible.

Models for turbines in two-phase flow have been proposed by Aya, Rouhani, Silverman, and Lahey[1,2,3,4]. The Lahey and Rouhani models are identical for steady state flow, but the Lahey model corrects for response during transients. The Lahey model is believed to be the most accurate model for twisted blade turbines available at this time for transient two-phase flow. The Rouhani equation for steady state two-phase flow is

$$u_f = \frac{u_t \left[\alpha S + (1 - \alpha) \frac{\rho_f}{\rho_g} \right]}{\alpha S^2 + (1 - \alpha) \frac{\rho_f}{\rho_g}} \qquad (3)$$

where

u_f = velocity of the liquid

u_t = velocity of the turbine indicated by the single-phase equation

α = void fraction (area of the steam divided by the total area)

S = velocity of the steam divided by the velocity of the water

ρ_f = density of the water

ρ_g = density of the steam.

3.2 Drag-Disc Equations

The single-phase coolant water temperature equation for the drag disc is

$$(\rho u^2)_{DD} = D_0 + D_1 V(t) \tag{4}$$

where

$(\rho u^2)_{DD}$ = momentum flux measured by the drag disc

$V(t)$ = voltage output of the drag disc.

The drag disc, used in the LOFT facility, is temperature sensitive; therefore, this equation must be modified as follows:

$$(\rho u^2)_{DD} = (Z_0 + Z_1 T) \frac{S_0 + S_1 T}{D_1} + (S_0 + S_1 T)\, V(t) \tag{5}$$

where

Z_0 = the zero offset from the zero offset temperature equation

Z_1 = change in the zero offset with temperature

T = temperature

S_0 = zero offset from the slope calibration temperature equation

S_1 = change in slope calibration with temperature

D_1 = full flow calibration at ambient temperature.

This equation, like that for the turbine, requires additional terms in two-phase flow. The output of the drag disc is

$$(\rho u^2)_{DD} = \rho_g u_g^2 + \rho_f u_f^2 (1 - \alpha) \qquad (6)$$

where

u_g = velocity of the steam.

This equation should be used in evaluating the effects of each phase in two-phase flow. Again, local void fraction is unknown; consequently, only the performance equation is used currently in LOFT.

4. PERFORMANCE AND RELIABILITY

The performance data used in this section are from a previous LOFT test, but the conclusions still apply. The statements on reliability are based on more recent test data.

4.1 Performance

The installation of the early drag-disc turbine transducer in LOFT was a single DTT located in the center of the pipe. When mass balance data from the DTT were compared with the mass expelled into the suppression tank, poor agreement was found. This discrepancy was due to either (a) an incorrect turbine or drag-disc model or (b) deviation from a flat velocity of momentum flux profile. A rake of three DTTs was then installed in the cold leg of the blowdown loop, as shown in Figure 15, to evaluate the profile. The following discusses the modeling of this rake when used to determine mass flow rate.

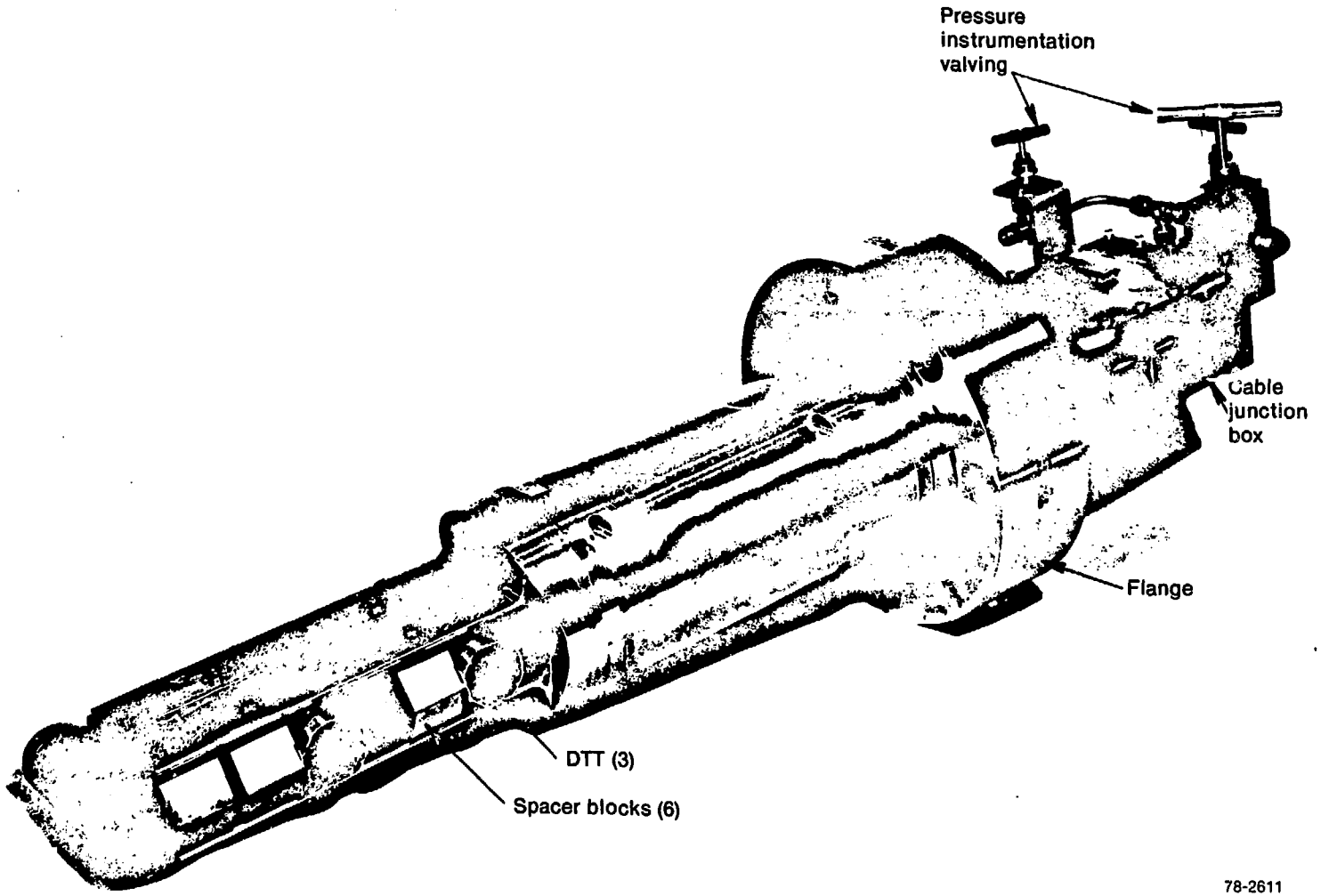

Fig. 15 DTT rake assembly.

The general approach in calculating mass flow rates using the DTT rake data is to estimate the density profile $\rho(\vec{r})$ and the velocity profile $u(\vec{r})$, multiply these two functions pointwise, and integrate (numerically) the product across the pipe area. $u(\vec{r})$ is estimated from the turbines, and $\rho(\vec{r})$ from the drag discs by using the turbine $u(\vec{r})$ estimate to remove the velocity dependence from the drag-disc readings.

Local fluid density values can be obtained from the DTT rake turbine and drag-disc readings. The $\rho(\vec{r})$ is estimated as a smooth function of the vertical coordinate only, and it passes exactly through the three points representing the three local measurements. This function is a half-cycle of a cosine function in each of the two regions between neighboring DTTs, and is constant outside of these regions. Some illustrative examples of $\rho(\vec{r})$ curves are given in Figure 16. This $\rho(\vec{r})$ function can be written in the form

$$\rho(\vec{r}) = \sum_{i=1}^{3} \rho_i f_i(y) \tag{7}$$

where ρ_i are the local density readings, y is the vertical coordinate, and the f_i are:

$$f_1(y) = \begin{cases} 1 & \text{for } 0 < y < y_1 \\ \frac{1}{2}\left[1 + \cos\left(\pi \frac{y - y_1}{y_2 - y_1}\right)\right] & \text{for } y_1 < y < y_2 \\ 0 & \text{otherwise} \end{cases}$$

$$f_2(y) = \begin{cases} \frac{1}{2}\ 1 - \cos\left(\pi \frac{y - y_1}{y_2 - y_1}\right) & \text{for } y_1 < y < y_2 \\ \frac{1}{2}\ 1 + \cos\left(\pi \frac{y - y_2}{y_2 - y_1}\right) & \text{for } y_2 < y < y_3 \\ 0 & \text{otherwise} \end{cases}$$

$$f_3(y) = \begin{cases} \frac{1}{2}\left[1 - \cos\left(\pi \frac{y - y_2}{y_3 - y_2}\right)\right] & \text{for } y_2 < y < y_3 \\ 1 & \text{for } y_3 < y < 2R \\ 0 & \text{otherwise.} \end{cases}$$

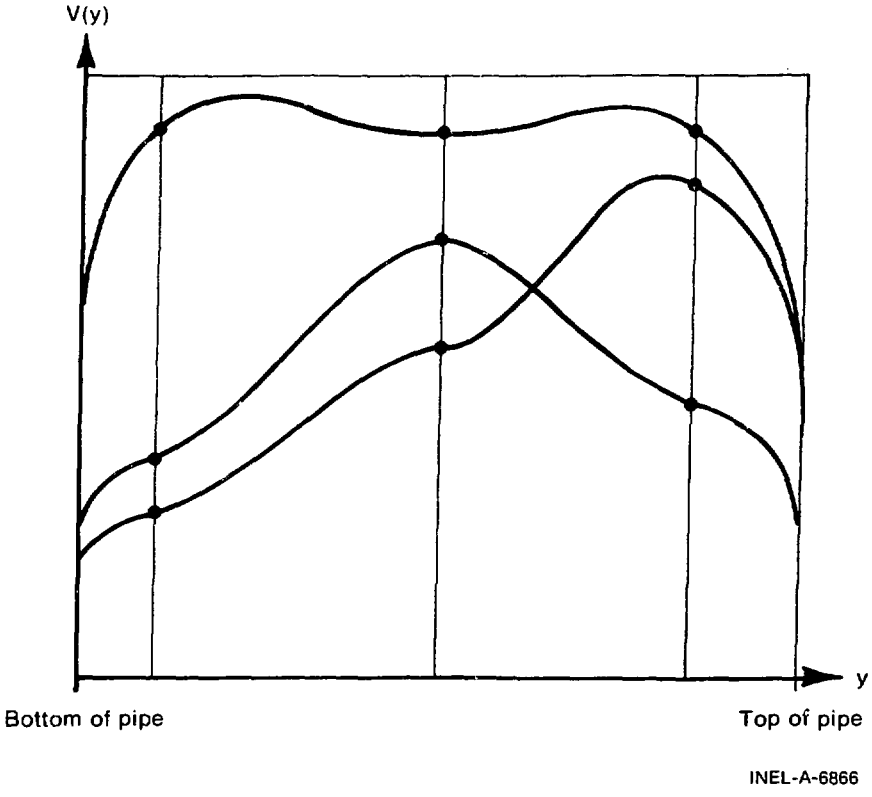

Fig. 16 Velocity profiles from drag-disc turbine transducer rake.

Local fluid velocity values can be obtained from the DTT rake turbines. Then $u(\vec{r})$ is estimated as the product of two functions: (a) a function of the vertical coordinate only, similar to the function used for estimating $\rho(\vec{r})$ from the DTT rake, and (b) the function, H(r), describing the Prandtl one-seventh power law profile in the radial direction. The velocity profile can be written in the form

$$u(\vec{r}) = H(r) \sum_{i=1}^{3} u_i \, g_i \, (y) \qquad (8)$$

where

$H(r) = (1 - r/R)^{1/7}$

u_i = the local velocity readings

$g_i(y) = f_i(y)/H(r_i)$

r_i = the radial coordinate of the ith local measurement.

The important characteristics of this velocity function are that it exactly fits the local velocity measurements and it is zero at the pipe wall. The actual velocity profiles may not conform well to the details of the Prandtl one-seventh power law, but this functional form seems to be as good as any a priori guess at the velocity profile. Some velocity profiles described by this function are shown in Figure 16.

The ultimate test of any velocity and momentum flux measurement in two-phase flow is how well the integrated mass flow rate is predicted. Table I compares the integrated mass flow rate obtained from different combinations. This table shows the results that have been consistent throughout the LOFT tests, that is, (a) the drag-disc turbine combination overpredicts mass flow rate, (b) the turbine densitometer combination underpredicts mass flow rate, and (c) the drag-disc densitometer combination yields approximately the correct answer. The densitometer model is believed to be correct and relatively insensitive to the model used[5].

The only remaining possible causes of the discrepancies in the mass flow calculations seem to be either the performance of the DTTs

TABLE I

INTEGRATED MASS FLOW AT 20 SECONDS DURING L1-4 TEST
IN THE COLD LEG OF THE BROKEN LOOP

Data Used	Mass (kg)
Turbine and drag disc	3319
Densitometer and drag disc	3044
Turbine and drag disc	3921
Average density and turbine	2653
Average density and drag disc	3046
Lahey transient turbine model and densitometer	3120

or the interpretation of the DTT data. One possible source of error in interpreting the DTT data is the lack of consideration of the rather slow response of the turbine under some conditions. To check on response, Lahey's transient turbine model was used to interpret the data. The velocity profile was assumed to be flat. The results indicate that the transient response correction gives some improvement (Table I).

4.2 Reliability

The reliability of the DTT has been continuously improved since its earliest design. The early drag-disc design experienced excessive sticking due to corrosion buildup and coil failure because of broken leads. The early turbine bearings would stick and bind due to crevice corrosion and the post stress relieving.

The current design has significantly increased the reliability of the DTT. The modular drag-disc transducer does not exhibit any sticking problem and a change in the fabrication process of the coil

has eliminated the coil failure. The modular turbine transducer, due to the self-aligning graphite bearings, has operated satisfactorily for over 2500 hours following long soak periods.

The DTT is not adversely affected by the LOFT pressures and temperatures, but excessive fluid vibrations have caused failures at the steam generator outlet and the reactor inlet. The major problem at these locations has been the inability to quantify vibration amplitudes and frequencies.

5. CONCLUSIONS

The DTT is undergoing continuous development. The current configuration appears to have solved the early problems of drag-disc stiction and turbine freezing. One reliability problem does exist. This problem is the vulnerability of the DTT to vibration.

The modeling or data handling of the turbine needs improvement. The transient tests at Wyle Laboratories should furnish insight to the correct handling of the turbine output. The drag disc gives the correct integrated mass flow rate when used with the densitometer. Problems of extrapolating from local to global do exist, but may not be as sensitive to modeling as originally thought.

6. REFERENCES

1. I. Aya, A Model to Calculate Mass Flow Rates and Other Quantities of Two-Phase Flow in a Pipe with a Densitometer, a Drag Disc, and a Turbine Meter, ORNL TM-47591 (November 1975).

2. Z. Rouhani, "Application of the Turbine Type Flowmeters in the Measurement of Steam Quality and Void," Paper D-6. Proceedings of Symposium on In-Core Instrumentation, Oslo, Norway, June 15-19, 1964, Institue for Atomenerg; Halden, Norway.

3. S. Silverman, Principles of Operation and Data Reduction Techniques for the LOFT Drag-Disc Turbine Transducer, TREE-NUREG-1109 (February 1977).

4. P. S. Kamath and R. T. Lahey, A Turbine Meter Evaluation Model for Two-Phase Transients, NES-459 (October 1977).

5. L. D. Goodrich and G. D. Lassann, "Mass Flow Instrumentation Performance During LOFT Nonnuclear Test Series," Twenty-Fourth International Instrumentation Symposium, May 1978.